

Quark model description of quasi-elastic pion knockout from the proton at JLAB

I.T. Obukhovskiy¹, D. Fedorov¹, A. M. Faessler²,
Th. Gutsche² and V. E. Lyubovitskiy²

¹ Institute of Nuclear Physics, Moscow State University,
Vorobiev Gory, Moscow 119899, Russia

² Institut für Theoretische Physik, Universität Tübingen,
Auf der Morgenstelle 14, D-72076 Tübingen, Germany

Abstract

The interference term between s - and t -pole contributions to the $p(e;e^0+)n$ cross section is evaluated on the basis of the constituent quark model. It is shown that the contribution of baryon s -poles can be modeled by a nonlocal extension of the Kroll-Rudermann contact term. This contribution is in a destructive interference with the pion t -pole that is essential to improve the description of recent JLab data at the invariant mass $W = 1.95$ GeV. Some predictions are made for a new JLab measurement at a higher value of $W = 3$ GeV.

PACS: 12.39.Fe, 12.39.Mk, 13.25.Jx, 13.40.Hg

Keywords: quark form factor, pion form factor, meson electroproduction.

1 Introduction

In Ref. [1] the JLab F²C Collaboration extracted from the data the charged pion form factor $F_\pi(Q^2)$ using a Regge model for high energy meson electroproduction [2]. Along with this the recent JLab data on the Rosenbluth separation of longitudinal and transverse cross sections for the reaction $p(e;e^0^+)n$ were presented.

The model [2] used for handling the recent data [1] interpolates between the low and higher momentum transfer regions and gives an economical description of the t - and s -dependence of the differential cross section. The procedure for reggeization according to [2] is quite natural for the t -pole diagrams pictured in Fig. 1a. However, the authors of Ref. [2] have been forced to add a nucleon-pole term (diagram in Fig. 1b) to the Regge amplitude to ensure gauge invariance. In general, the full sum of s -channel resonances taken with their proper form factors should be dual to the full sum of reggeon exchanges as it is schematically shown in Fig. 2 (see, e.g. the recent review [3]). But actually the form factors for the transitions $\pi^+ N \rightarrow N$ are only known with large uncertainties, and thus one can stay on a phenomenological level and use only some separate terms from both sums. Then the question about the other baryon-pole contributions to the amplitude (and to gauge invariance [4] as well) should be raised.

It is well known that s -pole resonances play an important role in pion photoproduction, but for pion electroproduction their contributions are suppressed at momentum transfers Q^2 above $1 \text{ GeV}^2/c^2$ due to the presence of the vertex form factors $F_{NN}(Q^2)$. Nevertheless, in the resonance region at invariant masses W up to 1.8 GeV they remain to be important [5]. At higher final state energies $W \approx 2 - 3 \text{ GeV}$ characteristic of the JLab measurements [1,6] there are no resonance peaks in the cross section, and thus a traditional resonance approach would not be an effective one. In that region one need not to account for the details of the intermediate nucleon excitations, and only a combined effect of all the s -channel contributions must be evaluated. In our opinion, for such evaluation a quark approach would be more convenient as it is schematically shown in Fig. 2 (the right diagram).

The aim of this letter is to show that an alternative (microscopic) description of quasi-elastic pion knockout from the proton (in the discussed region and including the $s(u)$ - and t -channel contributions) can be obtained on the basis of a constituent quark model (CQM). It implies that the constituent quark is an extended object and has its own electromagnetic form factor $F_q(Q^2) = 1/(1 + Q^2/\Lambda_q^2)$ [7]. The parameter Λ_q is believed to be set by the chiral symmetry scale $\Lambda_q \approx 4 \text{ fm}^{-1} \approx 1 \text{ GeV}$.

The t-pole contributions to the quasi-elastic pion knockout correspond to trivial quark diagrams shown in Fig. 3. Our hypothesis is that in the kinematical region discussed the full sum of nucleon and excited-nucleon s- and u-pole terms can be represented by the quark diagrams in Figs. 4a-f. Moreover, in the region of the pion t-pole, $t \approx m^2$, the sum of all the s- and u-channel contributions should be a small correction to the t-pole contribution $(t - m^2)^{-1}$: Therefore, one can neglect the highest order corrections $(m_q^2 - Q^2)^n$ represented by the diagrams in Figs. 4c-f in comparison to the dominant s- and u-pole terms in Figs. 4a and 4b.

In the CQM for the strong qq vertex form factor F_{qq} one can take the Fourier transform of the pion wave function (e.g. this can be shown [8] in terms of the 3P_0 model [9,10,11]). Then the quark amplitude for the s- or u-channel transition $\pi^+ q \rightarrow q^+ \pi^0$ becomes proportional to the product of two form factors, the strong F_{qq} and the electromagnetic F_q ones. In the considered region of large Q^2 and W , where we neglect a small $m_q^2 - Q^2$ corrections this product is equivalent to the pion electromagnetic form factor $F_\pi(Q^2) = F_q(Q^2) F_{qq}(Q^2)$ (see below in Section 3). As a result, in the considered kinematic region of quasi-elastic pion knockout both the t- and s(u)-contributions to the amplitude become proportional to a common form factor $F_\pi(Q^2)$ which can be factorized from the sum of t- and s(u)-pole diagram contributions. This feature is also consistent with gauge invariance of the calculated amplitude.

As a result we obtain an evaluation of a common effect of s- and u-pole contributions to the cross section. The overall contribution of such terms is Q^2 - and W -dependent and vanishes with increasing W and Q^2 in direct proportion to the factor $(\sqrt{Q^2} M_N - W^2) F_\pi(Q^2)$. Our evaluations show that for JLab data [1] at lower Q^2 (0.6 and 0.75 GeV²/c²) this contribution is important and cannot be neglected, while at higher values of Q^2 and W it becomes considerably smaller and practically invisible in the cross section at $W \gtrsim 3$ GeV. Unfortunately at small Q^2 , comparable with the cutoff parameter $Q^2 \approx 0.7$ GeV²/c² in NN vertices, one cannot exclude the direct contribution of intermediate baryon resonances to the cross section. Formally such small Q^2 are out of the region of the quasi-elastic kinematics and any evaluation based on a quasielastic approximation is questionable in this region. Only higher values $Q^2 \gtrsim 1.2$ GeV²/c² and $W \gtrsim 2.3$ GeV are appropriate for such evaluations. Results of a new JLab measurement at higher W should be more suitable as the parameter $(\sqrt{Q^2} M_N - W^2)$ characteristic of our approximation is safely small at $W \gtrsim 3$ GeV and we can properly predict the t-dependence of the cross section.

2 Pion-pole mechanism in terms of the constituent quark model

The possibility of describing the high-energy pion electroproduction in terms of the pion t-channel mechanism has been discussed in the literature over many years [12,13,14]. An important argument [14] is that the contribution of the s-channel diagrams in Fig.1b is suppressed by a factor $1=Q^4$ in comparison to the contribution of the t-channel diagrams in Fig.1a. Note that this argument was recently supported by new experimental data of MAMI [15] showing a soft Q^2 behavior of the transition form factors $N \rightarrow N$ at moderate Q^2 .

In Refs. [14,16,17], the pion t-channel diagram (i.e. the form factor F_{NN}) was calculated using the light-front dynamics. This made it possible to extract the strong NN form factor $F_{NN}(t)$ from comparison of a calculated cross section with the data. In contrast to those studies, in Ref. [8] the process $p(e;e^+)n$ was considered in the laboratory frame. In this case one is able to single out, in a natural way, the kinematical region where the recoil momentum of the final nucleon $P^0 = \sqrt{P_0^2 + k^2} \approx M_N + k^2/(2M_N)$ is small and where only the momentum $k^0 = q^0 + k^0$ of the knocked out meson is large. In that (quasi-elastic) region at $\sqrt{s} \approx 0.1 - 0.2 \text{ GeV}^2$ momentum $k = P - P^0$ transferred to the nucleon can be related to the 3-momentum \vec{k} . In particular, $k^0 \approx \sqrt{k^2 + M_N^2}$, and $t = k^2 \approx -k^2$. Therefore, both the initial $|N(P)\rangle$ and the final-state $|N(P^0)\rangle$ nucleons are nonrelativistic ones. In the CQM each of them can be described by a nonrelativistic wave function

$$|N_{3q}(P)\rangle = \int d^3x \, \psi_N(\vec{x}_1, \vec{x}_2) \chi^3 \chi^3 \chi^3 S_z; I_z \rangle \quad (1)$$

Here, $\chi^3 \chi^3 \chi^3 S_z; I_z \rangle$ is the color(C)-spin(S)-isospin(I) part and

$$\psi_N(\vec{x}_1, \vec{x}_2) = N e^{-\frac{x_1^2}{4b^2} - \frac{x_2^2}{2b^2}} \quad (2)$$

is the internal wave function normalized as $\int d^3x_1 d^3x_2 \psi_N^2(\vec{x}_1, \vec{x}_2) = 1$, where x_1 and x_2 are the Jacobi coordinates, N is a normalization constant and b is a dimensional parameter.

The t-pole amplitude for the $q \rightarrow q^0 +$ process on the i-th quark (Fig.3) is

$$M_{q(t)} = ie \hat{G}_{qq}^{(i)} \frac{F(Q^2)}{t - m^2} (k + k^0) ; \quad \hat{G}_{qq}^{(i)} = g_{qq}^{(i)} \gamma^{(i)} \cdot k \quad (3)$$

where $F(Q^2)$ is the pion electromagnetic form factor and $\hat{G}_{qq}^{(i)}$ is the qq vertex operator for the i-th quark, which is related to the pion-nucleon form factor $G_{NN}(k^2)$ as

$$G_{NN}(k^2) = k \sum_{i=1}^{X^3} \langle N_3(P^0) | \hat{G}_{qq}^{(i)} | N_3(P) \rangle = 5g_{qq} k e^{k^2 b^2 = 6} : \quad (4)$$

In the following, for convenience, we proceed with the normalized pion-nucleon form factor $F_{NN}(k^2) = G_{NN}(k^2)/G_{NN}(0)$ with $g_{NN} = G_{NN}(0)$. We use a simple form of the operator $\hat{G}_{qq}^{(i)}$ neglecting the momentum dependence since the exchanged pion and the constituent quarks are approximately on their mass shells.

The quark-level amplitude $M_{q(t)}$ gives rise to the t -pole matrix element for π^+ electroproduction from the nucleon

$$\begin{aligned} M_{N(t)} &= \langle N_3(P^0) | \sum_{i=1}^{X^3} M_{q(t)}^{(i)} | N_3(P) \rangle \\ &= i e g_{NN} F_{NN}(t) \frac{F(Q^2)}{t - m^2} (k + k^0) \quad k; \end{aligned} \quad (5)$$

which is proportional to the same strong form factor $F_{NN}(t)$ defined above. At $b = 0.6$ fm, which is a typical scale in the CQM, the matrix element (5) with the Gaussian strong form factor $F_{NN}(t)$ gives a reasonable description of the t -dependence of the differential cross sections in the JLab experiment (see, e.g., Ref. [8]). At small t , 0.2 GeV^2 this Gaussian is very close to the monopole form factor with $F_{NN}' = 0.7 \text{ GeV}$. A phenomenological analysis of the JLab data made in Ref. [18] has also demonstrated very similar values for F_{NN} .

3 Effective qq interaction

The above consideration implies large values of Q^2 , at which the diagonal and transition form factors, $F_{NN}(Q^2)$ and $F'_{NN}(Q^2)$, gradually vanish. In line with this assumption, in the previous section we have neglected the N^- - and N^0 -pole contributions in the same manner as in the work [8]. However, since the s - and u -channel quark contributions (Fig. 4a,b), which are required for gauge invariance, have not been taken into account, the results of such simple quark evaluation (dashed lines in Figs. 6a-d) are not so good in comparison with the Regge parametrization [2] used in Refs. [1,19] (dash-dotted lines in Figs. 6a-d).

Here we shall evaluate these contributions, starting from a nonlocal (nl) variant of the pseudoscalar qq coupling g_{qq}^{nl} , which differs from the local coupling g_{qq} by the presence of the quark form factor: $g_{qq}^{nl}(p^2) = g_{qq} F_{qq}(p^2)$. Hence, the vertex operator $\hat{G}_{qq}^{(i)}$ is modified accordingly. In this case the kinematics

is the following. Two particles, pion and ingoing (outgoing) quark, are on mass shell: $k^0 = m^2$, $p_i^2 = m_q^2$ ($p_i^{02} = m_q^2$), where $m_q = M_N/3$ is the mass of the constituent quark. But the intermediate quark with a large momentum $p_{i(s)}^0 = p_i + q$ ($p_{i(u)}^0 = p_i - q$) obtained by absorption (emission) of a momentum transfer from the should be considerably off its mass shell: $p_i^{02} \neq Q^2$, (see solid lines in Figs.4a and 5a or in Figs.4b and 5b).

The contribution of the quark diagrams in Figs.4a and 4b to the matrix element for absorption of the longitudinal virtual photon $\langle 0 | = \frac{1}{Q^2} f_{ij} q_j q_g$

$$M_{q(s+u)} = \left(\frac{p_i}{i} \frac{1}{2g_{qq}} F_q(Q^2) F_{qq}(Q^2) \right) \left(e_u \frac{1}{p_i^0 + k^0 m_q} + e_d \frac{1}{p_i^0 - k^0 m_q} \right) \quad (6)$$

was evaluated in the approximation $W^2 \ll Q^2; M_N^2$ where e_i ($i = u, d$) is the quark charge. We do not take into account the diagrams in Figs.4c-f since their contribution to the cross section include at least an additional small factor m_q^2/Q^2 . The shaded circle in Figs. 4c and 4d refers to the contribution of one- and two-gluon corrections, respectively.

In the considered region of a large momentum $k^0 = (k^0; k^0)$ with $k^0 = \frac{1}{m^2 + k^{02}} \cdot k^0$ and

$$k^0 j' \cdot j = \frac{1}{t} \frac{W^2 + Q^2 - M_N^2}{2M_N} + Q^2; \quad W^2 \ll Q^2; M_N^2 \quad (7)$$

transferred to the pion and of a small momentum $k = ft = (2M_N); k g' f_0; k g$ transferred to the nucleon we can omit all contributions to the amplitude proportional to small parameters

$$\frac{Q^2 - M_N^2}{W^2}; \frac{k \cdot j}{2M_N}; \frac{m_q^2}{W^2}; \frac{m^2}{M_N^2}; \dots \ll 1: \quad (8)$$

Then for deeply off-shell intermediate quarks in the diagrams in Fig. 5 one can write

$$p_{i(s)}^{02} \approx \frac{2M_N k_0^0}{3} \left(1 + \frac{3j_2 j_2}{M_N} \cos^2 \right) Q^2; \quad p_{i(u)}^{02} \approx p_{i(s)}^{02} - Q^2; \quad (9)$$

where j_2 is a relative momentum conjugated to the Jacobi coordinate j_2 , and $\cos^2 = \hat{k}^0 \cdot \hat{j}_2' \cdot \hat{q} \cdot \hat{j}_2$. By making use of the approximate equality $j_1 j_2 \approx$

$1 + Q^2 = (2q_0)$, which holds within the conditions (7) and (8), one obtains the approximation $(k^0 \approx \sqrt{Q^2} + \frac{1}{2}Q^2) \approx (k^0 \approx \sqrt{Q^2} + \frac{1}{2}Q^2)$ diagf \hat{q} ; $\hat{q}g$ useful for reducing the r.h.s. of Eq. (6) (the approximation implies that $k^0 \approx \hat{q}$, which is true for the forward pion knockout).

Finally, in the lowest order of expansion in the small parameters $M_N^2 = W^2$ and $Q^2 = W^2$ the matrix element (6) reduces to an effective qq interaction¹

$$M_{q(s+u)}^{(=0)} = M_{q(e)}^{(=0)} + O\left(\frac{Q^2}{W^2} \frac{M_N^2}{W^2}\right);$$

$$M_{q(e)}^{(=0)} = \frac{eg_{qq}}{2M_N} \frac{M_N^2}{\frac{1}{3}W^2} \frac{P \cdot \overline{Q}^2}{(1 + \frac{3j_{2j}}{M_N} \cos)} F_q(Q^2) F_{qq}(Q^2); \quad (10)$$

which is proportional to the product of quark form factors (note that the z_2 -dependent denominator, being integrated with Gaussian functions (1), introduces only a small correction to the integral, and thus we shall omit it in the final expression for the nucleon matrix element).

Some words should be added about the product of two quark form factors in the r.h.s. of Eq. (10). In the 3P_0 model one can take into account the inner qq structure of the pion introducing a pion wave function, e.g. in a Gaussian form. Then according to the 3P_0 model [8] the qq vertex is characterized by a form factor $F_{qq}(p^2) = e^{-p^2 b^2/8}$, where $p = p - p^0$ is the momentum transfer from the incoming to the outgoing quark and b is a radius of the Gaussian. On the other hand, in the CQM the vertex diagram pictured in Fig. 3b leads to a pion electromagnetic form factor $F_\pi(Q^2) = F_q(Q^2) e^{-Q^2 b^2/8}$. Hence, in the considered region of large Q^2 , where in s - and u -pole diagrams the momentum transfer in the qq vertex is approximately equal to $\sqrt{Q^2}$, we can use an approximate formula in our evaluations

$$F_q(Q^2) F_{qq}(p^2) \approx F_q(Q^2) F_{qq}(Q^2) \approx F_\pi(Q^2); \quad (11)$$

Eq. (11) is very useful to check gauge invariance of the sum t - and $s(u)$ -pole amplitudes in the final expression, where these amplitudes destructively interfere (see Sect. 4). For each of the amplitudes we have the same form factor $F_\pi(Q^2)$ which can be factorized out from the sum of amplitudes. The remainder is a sum of Feynman diagrams for point-like particles, which satisfies gauge invariance. It should be noted that gauge invariance can also be restored in the general case, if one uses different vertex form factors (see detailed discussion in Refs. [4,21]).

¹ At the photon point $Q^2 = 0$, $\hat{q} = f_0; \hat{n}_2 g$ and in the low-energy limit $k_0^0 \rightarrow m$ the same quark calculation gives exactly rise to the Kroll-Ruderman term [20] for the threshold pion photoproduction.

4 Longitudinal cross section: destructive interference of t - and $s(u)$ -pole terms.

We calculate the longitudinal differential cross section d_L/dt for quasi-elastic pion knockout taking into account both the t -pole diagram in Fig.3 and the s - and u -pole contribution (10)

$$\frac{d_L}{dt} = \frac{\overline{J_h^{(\lambda=0)} J}}{4(4\pi)^2 (W^2 - M_N^2) (W^2 - Q^2 - M_N^2)^2}; \quad (12)$$

where

$$\overline{J_h^{(\lambda=0)} J} = \frac{1}{2} \sum_{\text{spin}} \overline{J N_{3q}(P^0) J [M_{q(t)} + M_{q(s+u)}]^{(\lambda=0)} e^{i\frac{2}{3}k_z}^{(i)} J N_{3q}(P) J} \quad (13)$$

and compare the results to the JLab data [1] and to the Regge model [2] predictions [19] (see Fig. 6).

The CQM calculation of the right-hand side of Eq. (13) leads to a simple matrix element for a nonrelativistic nucleon wave function $N(\mathbf{p}_1; \mathbf{p}_2)$. Using Eqs. (5) and (10) we obtain in the laboratory frame the matrix element of the longitudinal hadron current for the transition $\pi^+ p \rightarrow \pi^+ n + \pi^+$:

$$J_h^{(0)} = i_N \frac{e g_{NN}}{2M_N} F(Q^2) \int d_1 d_2 e^{i\frac{2}{3}k_z} J N(\mathbf{p}_1; \mathbf{p}_2) J \quad (14)$$

$$\frac{2}{t - m^2} \frac{q_k}{m^2} + \frac{g_{b_1 NN}}{g_{NN}} \frac{g_{b_1}}{2M_N m_{b_1}} \frac{k_0}{Q^2} \frac{k \cdot \hat{q}}{t - m_{b_1}^2} \frac{k}{M_N} \frac{P \cdot \overline{Q}^2}{W^2} F_q^2(Q^2) \hat{q} :$$

Here the contribution of the b_1 -meson pole (i.e. the first orbital excitation of the pion with mass $m_{b_1} = 1.235 \text{ GeV}$) is also taken into account (the second term in the square brackets). However, the b_1 -pole contribution is small when compared to the ρ -pole contribution, which can be identified by comparison of the first and second terms in the r.h.s. of Eq. (14), which are proportional to the factors $g_{NN} = (t - m^2)$ and $(k_0 = m_{b_1}) g_{b_1 NN} = (t - m_{b_1}^2)$, respectively. The ρ -meson pole is not included as it does not contribute to the longitudinal part of the cross section (the $M1$ spin-flip amplitude $\pi^+ p \rightarrow \pi^+ n + \pi^+$ only contributes to the transverse part of the cross section where it is of prime importance [14,22,23]).

Here, the $b_1 NN$ and b_1 vertices are calculated on the basis of the 3P_0 model [9,10,11] with the technique described in Refs. [8,23]. The final expression for the b_1 vertex in the lab frame is compatible with the result of the nonrelativistic reduction of the general expression used in [2]

$$J_{b_1} = ie (\vec{k} \cdot \vec{q} - k'' \cdot q'') \frac{g_{b_1}}{m_{b_1}} F_{b_1}(Q^2; k^2; kq); \quad (15)$$

where g_{b_1} and F_{b_1} are free phenomenological values. For the $b_1 NN$ vertex we have the same situation.

The quark model calculation of the r.h.s. of Eq. (14) has the advantage that the parameters of the vertices g_{NN} , $g_{b_1 NN}$, g_{b_1} and their form factors $F_{NN}(t)$, $F_{b_1 NN}(t)$, $F_{b_1}(Q^2)$ are not free, but related to each other by the following relations:

1) The integral part of Eq. (14) defines a nonrelativistic vertex form factor $F_{m NN}(t) = F_{NN}(t) = F_{b_1 NN}(t)$ common to all three terms in Eq. (14).

2) The relative phases of all the amplitudes in the r.h.s of Eq. (14) are fixed by the results of quark model calculations. Therefore, the negative sign of the interference term between t - and s -pole contributions (the destructive interference) is unambiguously determined: the spin average of the product of the first term in the squared bracket of Eq. (14) with the third one has a negative value: $1 = 2 \sum_{S_z S_z^0} \langle S_z^0 j - \hat{k} \cdot \hat{p}_z \rangle \langle S_z j - \hat{q} \cdot \hat{p}_z^0 \rangle = \cos(\theta_q)$: Recall that $\cos(\theta_q) \approx -1$ in the quasielastic pion knockout kinematics, where \vec{k} is the momentum of the nucleon-spectator in the lab frame.

3) Note that in the discussed kinematical region the final results for the cross section practically do not depend on the b_1 -pole contribution. Nevertheless, for completeness we also summarize the quark constraints on the values of $g_{b_1 NN}$, g_{b_1} and $F_{b_1}(Q^2)$. The e.m. form factors $F(Q^2)$ and $F_{b_1}(Q^2)$, which correspond to the quark diagram in Fig. 3b, should be very similar to each other; e.g. they have the same expression in the CQM:

$$F(Q^2) = F_q(Q^2) e^{Q^2 b^2/8}; \quad F_{b_1}(Q^2) = F_q(Q^2) e^{Q^2 b_{b_1}^2/8}; \quad (16)$$

where b and b_{b_1} are the quark radii of π - and b_1 -mesons correspondingly, $F_q(Q^2) = \frac{2}{q} = (\frac{2}{q} + Q^2)$. As evident from Fig. 7 a description of $F(Q^2)$ by Eq. (16) is very realistic for $b = 0.3$ fm and $\frac{2}{q} = 0.95$ GeV²/c² in a large region close to the characteristic value of $Q^2 \approx M_N^2$, and thus, starting from the similarity of F_{b_1} and F in Eqs. (16), we use for $F_{b_1}(Q^2)$ the same parametrization as for $F(Q^2)$. The coupling constant g_{b_1} could also be evaluated on the basis of the CQM diagram of Fig. 3b as a matrix element of an orbital $P \rightarrow S$ transition, but we use a more realistic value of $g_{b_1} = 0.79$, which gives the experimental radiative decay width $\Gamma_{b_1 \rightarrow \pi \gamma}$.

4) The 3P_0 model also fixes the relation between the $b_1 NN$ and NN couplings (see Refs. [8,23] for details): $g_{b_1 NN} = g_{NN} = \frac{m_{b_1}}{m}$. It implies $g_{b_1 NN} = 40$ which is used in our evaluations.

5 Results and outlook

In our calculation we use a standard (monopole-like) representation for the pion charge form factor with $f_\pi^2 = 0.54 \text{ GeV}^2/c^2$ which is close to the recent theoretical evaluation [24,25] and correlates well with the recent JLab data [1]. We vary only one free parameter in the standard representation of the strong NN form factor $F_{NN}(Q^2) = f_{NN}^2/(f_{NN}^2 + Q^2)$ where the range $f_{NN} = 0.6 - 0.7 \text{ GeV}/c$ corresponds to the reasonable value $b = 0.5 - 0.6 \text{ fm}$ for the radius of the three-quark configuration s^3 used in the CQM nucleon wave function (1). At realistic values of $f_{NN} = 0.75 \text{ GeV}/c$ and $g_{NN} = 13.5$ our results (the solid lines in Figs. 6a-d) are in a better agreement with the data [1] than the simplified model [8] taking into account only the pion t-pole not satisfying gauge invariance.

In our calculation we model the contribution of baryon resonances in the s- and u-channel by a nonlocal extension of the Kroll-Rudermann contact term. This contribution is negative, which is essential to improve the description of the measured cross section. At intermediate values of $Q^2 \approx 1 \text{ GeV}^2/c^2$, which correspond to a quasi-elastic mechanism of pion knockout, the calculated cross section is close to the experimental data. At smaller $Q^2 < 0.7 \text{ GeV}^2/c^2$ our results are close to the cross section calculated in Ref [19] (dash-dotted lines) on the basis of a model [2] which takes into account both the Reggeon-pole exchange and the nucleon-pole contribution. Recall that in Ref. [1] a phenomenological background term is fitted to describe the data at small Q^2 .

For a new JLab measurement of d_L/dt at higher invariant mass (the data analysis is presently underway) in Fig. 8 we give our prediction for the t-dependence of the cross section at $W = 3 \text{ GeV}$ and $Q^2 = 1 - 2 \text{ GeV}^2/c^2$. Here we use fixed (above defined) parameters of the model. Because of the large value of W the contribution of the effective contact term (10), which is proportional to the factor $f_{NN}^2/Q^2 M_N^2 = W^2$, becomes too small and practically invisible in the cross section (a small difference between the solid and the dashed curves in Fig. 8).

Our calculations show that the longitudinal cross section practically does not depend on the contribution of the b_1 -meson pole, and thus the data [1] cannot constrain the $b_1 NN$ and b_1 vertices. In contrast, data on the transverse cross section should be critically dependent on the ρ -pole contribution and on the spin- ρ amplitude. This was first shown in Ref. [14] and then supported in Refs. [22,23]. We have preliminary results in the above model, which confirm this statement. On the other hand, a Regge description [2] of the transverse cross section is not as good as for the longitudinal case. It is possible that microscopic models are in competition with the Regge phenomenology in this area. In future we intend to analyze new data on the transverse cross section

of pion quasi-elastic knockout $d_T = dt$ at higher invariant mass and momentum transfers in terms of the above model containing the form factors and coupling constants not only for the NN and πNN vertices, but also for the NN and πNN ones.

Acknowledgements

The authors thank Profs. V.G. Neudatchin and N.P. Yudin for fruitful discussions and criticism. This work was supported by the DFG under contracts FA 67/25-3 and GRK 683 and the DFG grant 436 RUS 113/790/. This research is also part of the EU Integrated Infrastructure Initiative Hadron-physics project under contract number R II3-CT-2004-506078, President grant of Russia "Scientific Schools" No. 1743.2003 and grants of Russia RFBR No. 05-02-04000, 05-02-17394 and 03-02-17394.

References

- [1] J. Volmer et al. [The Jefferson Lab F² Collaboration], Phys. Rev. Lett. 86 (2001) 1713 [arXiv:nuclex/0010009].
- [2] M. Guidal, J.-M. Laget and M. Vanderhaeghen, Nucl. Phys. A 627 (1997) 645; M. Vanderhaeghen, M. Guidal and J.-M. Laget, Phys. Rev. C 57 (1998) 1454.
- [3] W. Melnitchouk, R. Ent and C. Keppel, Phys. Rept. 406 (2005) 127 [arXiv:hep-ph/0501217].
- [4] J.H. Koch, V. Pascalutsa and S. Scherer, Phys. Rev. C 65 (2002) 045202.
- [5] D. Drechsel, O. Hanstein, S. S. Kamalov and L. Tiator, Nucl. Phys. A 645 (1999) 145 [arXiv:nucleth/9807001].
- [6] G. Huber, D. Mack and H. Block, JLab experiment E01-004 (2003); E. J. Beise, AIP Conf. Proc. 698 (2004) 23 [Nucl. Phys. A 751 (2005) 167].
- [7] F. Cardarelli, I. L. G. rach, I. M. Narodetsky, E. Pace, G. Salme and S. Simula, Phys. Rev. D 53 (1996) 6682 [arXiv:nucleth/9507038].
- [8] V. G. Neudatchin, I. T. Obukhovsky, L. L. Sviridova and N. P. Yudin, Nucl. Phys. A 739 (2004) 124 [arXiv:nucleth/0401062].
- [9] A. Le Yaouanc, L. Oliver, O. Pene and J. C. Raynal, Hadron Transitions in the Quark Model (Gordon and Breach Science Publishers, N.Y., 1988).
- [10] F. Cano, P. Gonzalez, S. Noguera and B. Desplanques, Nucl. Phys. A 603 (1996) 257 [arXiv:nucleth/9606038].
- [11] E. S. Aclah, T. Barnes and E. S. Swanson, Phys. Rev. D 54 (1996) 6811 [arXiv:hep-ph/9604355].

- [12] F. Gutbrod and G. Kramer, Nucl. Phys. B 49 (1972) 461.
- [13] A. Actor, J. G. Komer and I. Bender, Nuovo Cim. A 24 (1974) 369.
- [14] J. Speth and V. R. Zoller, Phys. Lett. B 351 (1995) 533 [[arXiv:hep-ph/9502382](#)].
- [15] A. Liesenfeld et al. [A1 Collaboration], Phys. Lett. B 468 (1999) 20 [[arXiv:nuclex/9911003](#)].
- [16] J. Speth and A. W. Thomas, Adv. Nucl. Phys. 24 (1997) 83.
- [17] N. N. Nikolaev, A. Szczurek and V. R. Zoller, Z. Phys. A 349 (1994) 59.
- [18] K. G. Vansyoc, Ph.D. thesis, Old Dominion University, Norfolk, 1998 (unpublished).
- [19] J. Volmer, Ph.D. thesis, Vrije Universiteit, Amsterdam, 2000 (unpublished).
- [20] N. M. Kroll, M. A. Rudermann Phys. Rev. 93 (1954) 233.
- [21] F. Gross and D. O. Riska, Phys. Rev. C 36 (1987) 1928.
- [22] N. P. Yudin, L. L. Sviridova, and V. G. Neudatchin, Phys. At. Nucl. 61 (1998) 1577.
- [23] I. T. Obukhovskiy, V. G. Neudatchin, L. L. Sviridova and N. P. Yudin, Phys. At. Nucl. 68 (2005) 1381.
- [24] P. Maris and P. C. Tandy, Phys. Rev. C 62 (2000) 055204 [[arXiv:nucloth/0005015](#)].
- [25] A. Faessler, T. Gutsche, M. A. Ivanov, V. E. Lyubovitskij and P. Wang, Phys. Rev. D 68 (2003) 014011 [[arXiv:hep-ph/0304031](#)].

LIST OF FIGURES

Fig.1: Pole diagrams for π^+ electroproduction on the proton: (a) meson t-poles, (b) baryon s-poles.

Fig.2: Dual description of the $\pi^+ N \rightarrow N$ process in terms of a sum over s-channel resonances $N^*(s)$ and in terms of t-channel Reggeon exchanges $\alpha_j(t)$ corresponding to quark exchange diagrams [3].

Fig.3: Quark diagrams for the t-channel mechanism of pion knockout.

Fig.4: Quark diagrams for the s- and u-channel mechanism of pion knockout. Thick lines indicate large Q^2 transition.

Fig.5: Sum of quark s- and u-pole diagrams reduced to an effective contact term.

Fig.6: Longitudinal cross section d_L/dt for the $p(e;e^0\pi^+)n$ process. Dashed lines: the pion t-pole only ($\alpha_{NN} = 0.75 \text{ GeV}$). Solid lines: meson t-poles + quark s- and u-poles with a quark form factor ($\alpha_q = 0.95 \text{ GeV}$). Pointed lines: the same as solid ones but without a quark form factor. Dash dotted lines: results of Refs. [1,19] for a Regge model [2]. Experimental data from Ref. [1]: (a) $Q^2 = 0.6$, (b) 0.75, (c) 1.0 and (d) $1.6 \text{ GeV}^2/c^2$; $W = 1.95 \text{ GeV}$.

Fig.7: The pion charge form factor $F(Q^2)$ in the CQM compared to the monopole representation ($\alpha^2 = 0.54 \text{ GeV}^2/c^2$).

Fig.8: Predicted cross sections d_L/dt for new JLab measurements at a higher value of invariant mass with $W = 3 \text{ GeV}$ [6]. Curves from the upper to the lower ones correspond to the values $Q^2 = 1, 1.5$, and $2 \text{ GeV}^2/c^2$. The solid and dashed curves are defined in Fig. 6. At small t the curves are limited by a kinematical border.

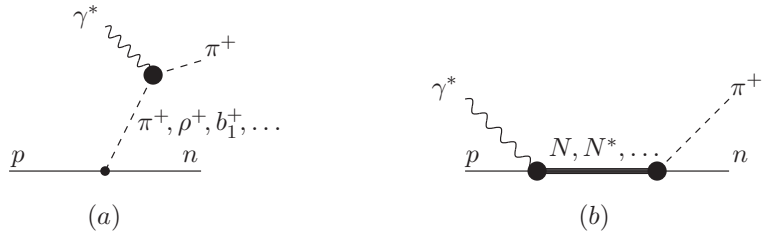


Fig.1

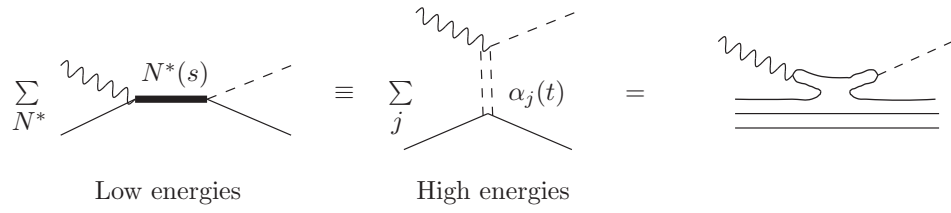


Fig.2

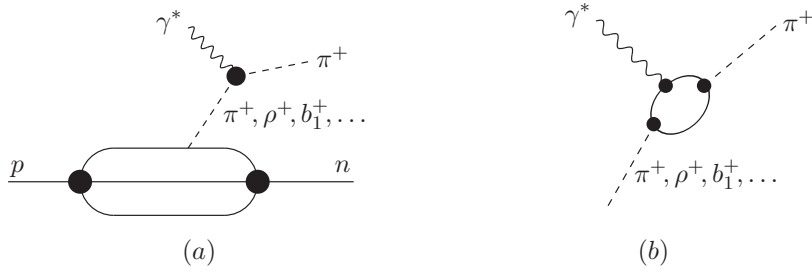


Fig.3

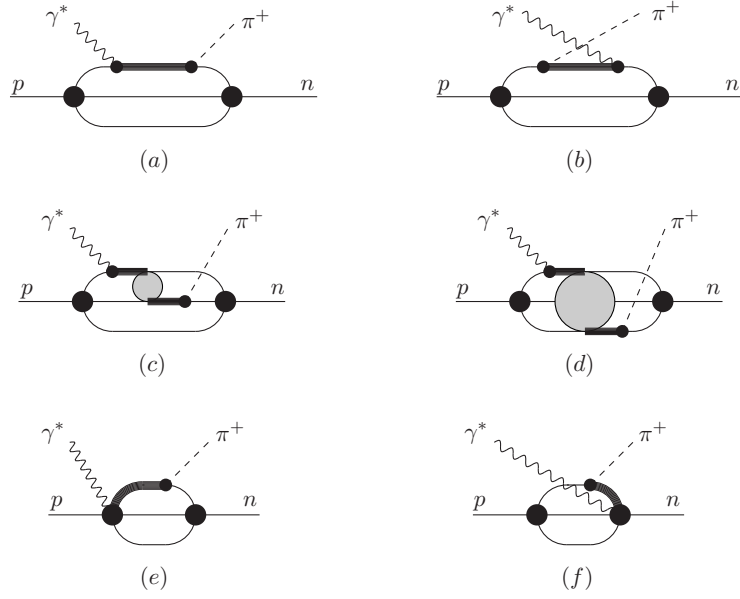


Fig.4

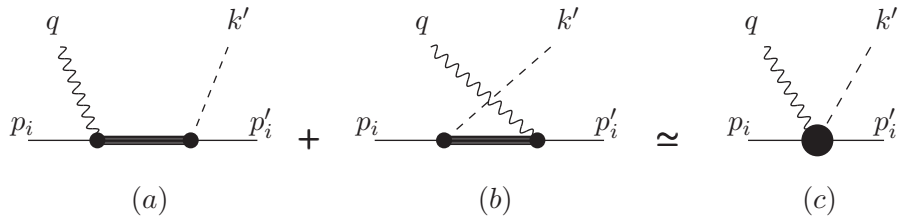


Fig.5

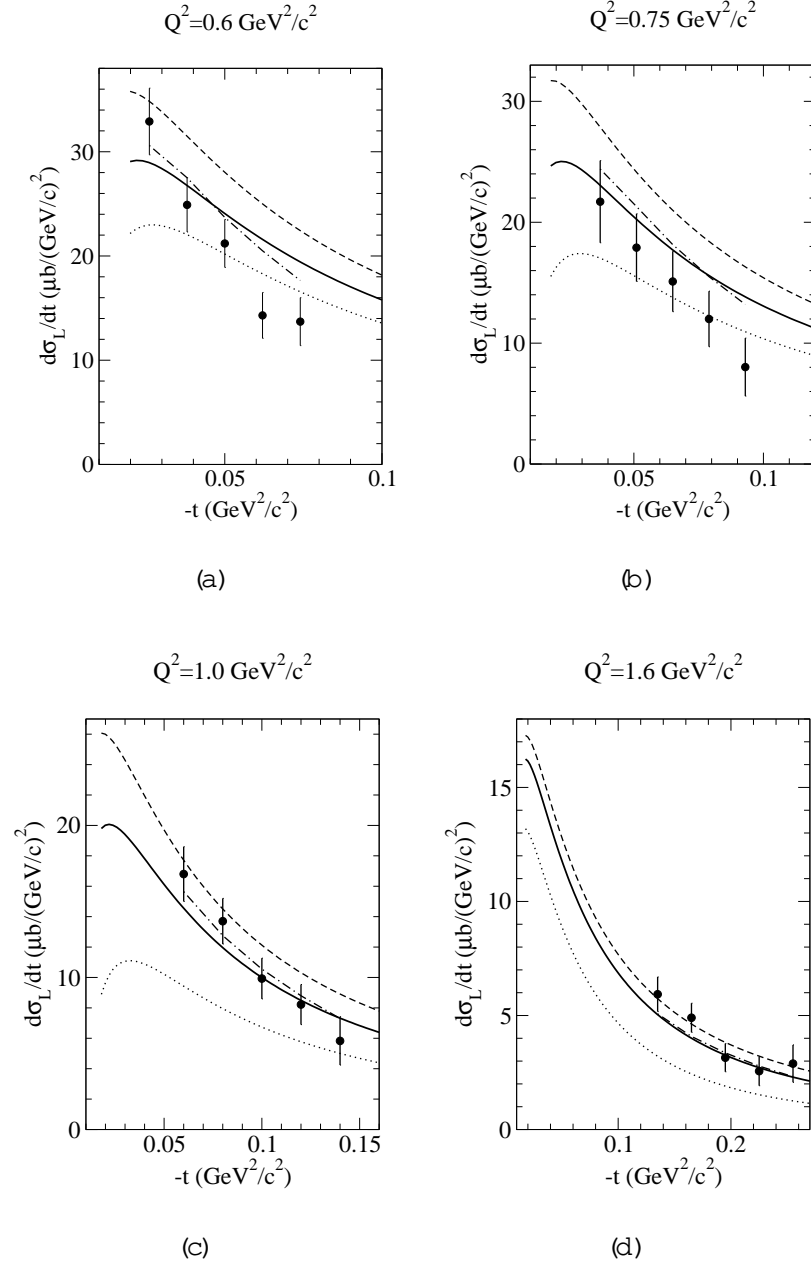


Fig.6

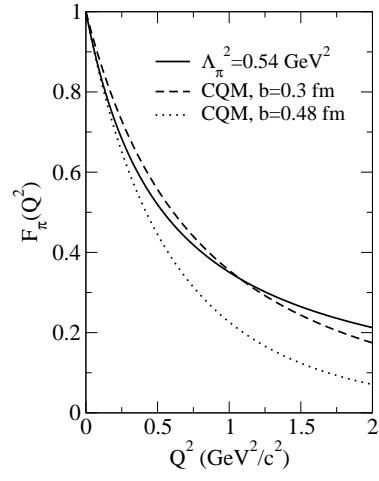


Fig.7

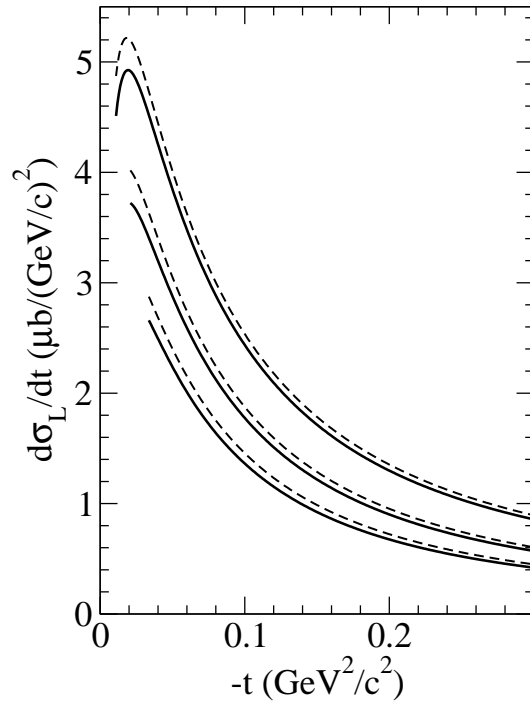


Fig.8